Title

Multi-Decadal Dynamics of Wetland Methane Emissions Revealed by Knowledge-Guided Machine Learning

Journal

Global Change Biology, 32(5)

ISSN

1354-1013

Authors

Zhu, Qing
Arndt, Kyle A
Yuan, Kunxiaojia
et al.

Publication Date

2026-05-01

DOI

10.1111/gcb.70899

Global Change Biology
WILEY
SPECIAL ISSUE FLUXNET Towards a Better Understanding of Global GHG Fluxes
Global Change Biology

RESEARCH ARTICLE OPEN ACCESS

Multi-Decadal Dynamics of Wetland Methane Emissions Revealed by Knowledge-Guided Machine Learning

Qing Zhu[1] | Kyle A. Arndt[2] | Kunxiaojia Yuan[1,3] | Fa Li[4,5] | Qing Ying[6,7] | Licheng Liu[8,9] | Eric Ward[6,7] | Avni Malhotra[10] | Jianqiu Zheng[10] | Fenghui Yuan[8] | Sparkle L. Malone[11] | Gavin McNicol[12] | Sara H. Knox[13] | William J. Riley[1] | Margaret S. Torn[1] | Shuo Chen[14] | Ben Riddell-Young[15,16] | Youmi Oh[15,16] | Lori Bruhwiler[16]

[1]Climate and Ecosystem Sciences Division, Lawrence Berkeley National Laboratory, Berkeley, California, USA | [2]Woodwell Climate Research Center, Falmouth, Massachusetts, USA | [3]Department of Earth and Atmospheric Sciences, University of Houston, Houston, Texas, USA | [4]Department of Earth System Science, Stanford University, Stanford, California, USA | [5]Department of Earth and Planetary Sciences, Jackson School of Geosciences, The University of Texas at Austin, Austin, Texas, USA | [6]Earth System Science Interdisciplinary Center, University of Maryland, College Park, Maryland, USA | [7]Biospheric Sciences Laboratory, National Aeronautics and Space Administration Goddard Space Flight Center, Greenbelt, Maryland, USA | [8]University of Minnesota, Minneapolis, Minnesota, USA | [9]University of Wisconsin-Madison, Madison, Wisconsin, USA | [10]Biological Sciences Division, Pacific Northwest National Laboratory, Richland, Washington, USA | [11]Yale School of the Environment, Yale University, New Haven, Connecticut, USA | [12]Department of Earth and Environmental Sciences, University of Illinois Chicago, Chicago, Illinois, USA | [13]Department of Geography, McGill University, Montreal, Quebec, Canada | [14]Department of Earth, Atmospheric, and Planetary Sciences, Purdue University, West Lafayette, Indiana, USA | [15]Cooperative Institute for Research in Environmental Sciences, University of Colorado, Boulder, Colorado, USA | [16]Global Monitoring Laboratory, NOAA, Boulder, Colorado, USA

Correspondence: Qing Zhu (qzhu@lbl.gov)

Received: 20 October 2025 | **Revised:** 23 March 2026 | **Accepted:** 31 March 2026

Keywords: AmeriFlux sites | knowledge-guided machine learning | long-term trend and variability | methane emission | wetland

ABSTRACT

Measurement of methane fluxes (FCH_4) from natural systems, such as wetlands, has lagged far behind carbon dioxide fluxes. Short and fragmented wetland FCH_4 data limit our ability to assess its long-term dynamics and potential climate feedbacks. Extrapolating short-term FCH_4 records to recent decades remains challenging for both process-based models and data-driven machine learning (ML) approaches. Here, we develop a knowledge-guided ML framework that integrates eddy covariance (EC) FCH_4 observations, field warming experiments, and biogeochemical knowledge to reconstruct the long-term FCH_4 budgets and trends. Focusing on the 11 longest EC monitoring sites in the AmeriFlux network, we found considerable variability in multi-decadal trends of wetland FCH_4, with increases up to 14% per decade from 2000 to 2024. We also found that the strength of these increasing trends declines from high to low latitudes, highlighting the vulnerability of northern wetlands. This work presents novel and robust reconstructions of long-term wetland FCH_4, offering critical benchmark datasets for bottom-up ecosystem models and advancing fundamental understanding of wetland biogeochemistry.

1 | Introduction

Eddy-covariance (EC) observations (Baldocchi 2014) deliver high-frequency measurements of ecosystem-scale CH_4 fluxes (FCH_4), and the EC network has significantly expanded FCH_4 measurements in recent decades (Knox et al. 2019). Currently, the FLUXNET-CH_4 community product (Delwiche et al. 2021) offers harmonized, gap-filled FCH_4 time series for 79 sites, emphasizing data quality through robust QA/QC, friction velocity filtering, and innovative gap-filling methods (Knox et al. 2019), aiming to enhance the accuracy of monthly and annual budget estimates. These EC sites represent diverse wetland habitats from arctic to tropical regions, facilitating comprehensive analyses of FCH_4 drivers (Knox et al. 2021), spatial representativeness (Watts et al. 2026; Zhu et al. 2024), upscaling (McNicol et al. 2023; Yuan et al. 2024), and large-scale model-data comparisons (Chang et al. 2023). Recent studies have also leveraged these datasets to refine bottom-up global wetland FCH_4 estimates over seasonal to decadal scales (Chen et al. 2025; Chinta et al. 2024; Yazbeck et al. 2025; Zhu et al. 2025).

Nevertheless, existing FCH_4 records from EC measurements face important limitations from short temporal coverage. Many wetland EC sites are characterized by short deployment durations (months to a few years), intermittent operation, and substantial data gaps due to instrument failures or low turbulence conditions (Delwiche et al. 2021; Knox et al. 2019). The limited temporal extent of most EC records (often <5 years) poses challenges for characterizing long-term dynamics and detecting climate-driven trends in wetland CH_4 emissions. Short and discontinuous EC data require approaches that introduce robust out-of-sample extrapolation. As a result, while EC observations are valuable for quantifying ecosystem-scale wetland FCH_4, their limited temporal coverage constrains their ability to understand long-term dynamics under changing environmental conditions.

Multi-decadal knowledge of wetland FCH_4 is essential for understanding the role of wetlands in the global carbon cycle and their responses and feedbacks to long-term (>20 years) climate change (Ciais et al. 2026). As the largest natural source of CH_4, wetland FCH_4 is strongly regulated by temperature, hydrology, and vegetation dynamics. Reconstructing site-level long-term wetland FCH_4 budgets enables us to quantify interannual-to-decadal variability, assess responses to past climate conditions, and improve predictions of future feedbacks under warming scenarios (Nisbet et al. 2019; Saunois et al. 2020). Here, we define "reconstruct" to be a hindcast of long-term daily in situ FCH_4 using a model trained on sparse EC data.

These reconstructions also provide benchmarks for evaluating bottom-up and top-down models, reducing uncertainties in large-scale CH_4 cycling across wetland types and climatic regions. Multi-decadal datasets are also crucial for informing mitigation strategies. Accurately characterizing the timing, magnitude, and spatial patterns of emissions can help design targeted interventions, assess the effectiveness of wetland conservation and restoration activities (Ma et al. 2024; Schuster et al. 2024).

Traditional modeling approaches for wetland FCH_4 face several critical challenges for long-term reconstruction. Bottom-up process-based models often mechanistically capture the functional response of FCH_4 to environmental changes; however, they struggle to accurately capture the magnitude and variability at the site level due to incomplete representations of mechanisms and biases when applied across diverse wetland ecosystems (Zhang et al. 2025), particularly when underdetermined location-specific parameters are used (Chang et al. 2023).

Similarly, conventional machine learning (ML) models can achieve high predictive accuracy, but their performance is often limited to the training window. They generally struggle to extrapolate to out-of-sample conditions, such as responding realistically to climate-driven changes (Beucler et al. 2024). Due to their black-box nature, these models often lack physical consistency (Feron et al. 2024) and struggle to account for environmental changes that may not have been represented in the limited training data. As a result, the lack of a physical basis in traditional ML models makes it difficult to trust their outputs for long-term predictions (Yuan et al. 2022). There is a growing need for models that combine predictive power with physical consistency and interpretability, enabling reliable estimation of site-level emissions, a mechanistic understanding of environmental controls, and robust long-term reconstructions under changing climate conditions (Liu et al. 2024).

The objective of this research is to develop a knowledge-guided machine learning framework for reconstructing multi-decadal (2000–2024) site-level wetland FCH_4. This approach integrates in situ EC observations, field warming experiments, remote sensing, and mechanistic knowledge to produce robust reconstructions of FCH_4 across diverse wetland ecosystems. The study is driven by three key scientific questions: (1) How have wetland FCH_4 evolved over the past two decades across different climatic regions and ecosystem types? (2) Are there statistically significant long-term trends, breakpoints, or shifts in emission intensity? (3) What are the dominant environmental and biological drivers that control long-term trends in wetland FCH_4? By addressing these questions, we aim to improve the mechanistic understanding and predictive capacity of wetland biogeochemistry models and provide critical information for climate mitigation and wetland management strategies.

2 | Methodology

2.1 | Flux Measurements and Supporting Data

We compiled eddy-covariance (EC) site measurements of wetland FCH_4 from the AmeriFlux database (Table 1, last accessed 08/01/2025), focusing on natural and unmanaged wetlands. We chose the top 11 longest records of FCH_4 for the current analysis to ensure robust long-term coverage and enable temporal analysis from annual to decadal scales. As a result, sites with more than 8 years of FCH_4 observations were included. The flux data were further processed following FLUXNET protocols, including despiking, friction velocity (u*) filtering, and comprehensive quality assurance/quality control (QA/QC) procedures to remove unreliable or low-turbulence measurements (Delwiche et al. 2021), resulting in processed daily variables of FCH_4, Gross Primary Productivity (GPP), air temperature, precipitation, incident shortwave radiation, wind speed, relative humidity, and air pressure.

Soil thermal and hydrological properties (i.e., soil temperature and water table depth) are not always available at EC sites. As a result, we used 3, 7, and 30-day moving averages of air temperature as a proxy for the dynamics of soil temperature, which may be lagged from air temperature (Feron et al. 2024). This approach aligns with a global analysis showing air temperature and soil temperature are tightly coupled and explain similar variability in soil respiration (Jian et al. 2022). Similarly, we used 3, 7, and 30-day cumulative precipitation as proxies for soil water conditions (Feron et al. 2024). We also utilized MODIS surface reflectance data (Red, Green, Blue, NIR1, NIR2, SWIR1, and SWIR2) to consider possible disturbance and land cover changes at the EC tower locations (Wang et al. 2018).

TABLE 1 | Selected EC sites of natural freshwater wetlands (see locations in Figure 2).

Site	Name	Type	Lat	Lon	Years	MAT (°C)	MAP (mm)	References
US-ICs	Imnavait Creek Watershed Wet Sedge Tundra	Wet tundra	68.60	−149.31	2007–2024	−9.2	496	Euskirchen et al. (2025)
US-NGB	NGEE-Arctic Barrow	Wet tundra	71.28	−156.61	2012–2019	−8.9	262	Torn and Dengel (2023)
US-BZB	Bonanza Creek Thermokarst Bog	Bog	64.69	−148.32	2011–2024	−1.7	417	Euskirchen (2025a)
US-BZF	Bonanza Creek Rich Fen	Fen	64.70	−148.31	2011–2024	−1.7	417	Euskirchen (2025b)
US-MBP[a]	Marcell Bog Lake Fen	Fen	47.50	−93.48	2009–2024	5.1	791	Roman et al. (2025)
US-Los	Lost Creek	Fen	46.08	−89.97	2000–2024	5.6	900	Desai (2025)
US-ALQ	Allequash Creek Site	Fen	46.03	−89.60	2015–2024	5.6	900	Olson (2025)
US-OWC	Old Woman Creek	Marsh	41.37	−82.51	2015–2024	10.8	1090	Bohrer and McMurray (2025)
US-NC4[a]	NC Alligator River	Swamp	35.78	−75.90	2009–2025	17.3	1233	Noormets et al. (2024)
US-LA2	Salvador WMA Freshwater Marsh	Marsh	29.85	−90.28	2011–2023	21	1452	Ward et al. (2025)
US-Elm	Everglades (long hydroperiod marsh)	Marsh	25.55	−80.78	2008–2024	24.3	1359	Starr and Oberbauer (2025)

[a]Did not pass the Augmented Dickey-Fuller (ADF) stability test for the site's NDVI time series, indicating disturbances during the study period.

Further, we calculated NDVI (Normalized Difference Vegetation Index) using MODIS reflectance at each site and employed the Augmented Dickey-Fuller (ADF) test to determine whether the mean and variance of the NDVI time series are stationary or non-stationary over time. As highlighted in Table 1, US-MBP and US-NC4 did not pass the stability test, indicating that their non-stationarity is likely due to significant disturbances, such as drought or land use changes. Since we included the original MODIS reflectance as predictors, such non-stationary changes are expected to have been accounted.

2.2 | Development of a Knowledge-Guided Machine Learning Framework

To reconstruct multi-decadal wetland FCH_4, we developed a knowledge-guided machine learning (KGML) framework that integrated EC flux measurements and process-based knowledge. The model architecture combined conventional ML algorithms (a neural network, see Table S1 for configuration) with knowledge constraints (through the loss function) derived from process understanding of how wetland FCH_4 responds to environmental and biological drivers (Jin et al. 2026).

The neural network architecture consists of an input layer that accommodates 19 features, followed by multiple hidden layers, which can vary in number between 5 and 10 layers, depending on model hyperparameter tuning. Each hidden layer has either 64 or 128 neurons and employs the ReLU (Rectified Linear Unit) activation function to introduce non-linearity into the model. The network is fully-connected and linked to the output layer that generates the final predictions of FCH_4. To enhance the model's performance and prevent overfitting, we incorporate dropout layers and batch normalization throughout the architecture. The number of hidden layers and neurons in each layer is treated as a hyperparameter, allowing for optimization during the model training process to achieve the best predictability. Overall, this architecture is designed to effectively capture the complex relationships within the dataset while maintaining physical robustness via knowledge constraints (Section 2.2.1) and producing realistic responses under varying environmental conditions.

2.2.1 | Knowledge Constraints

Key knowledge constraints were derived from process-based models. We surveyed governing equations of FCH_4, in terms of their temperature response and substrate control, based on bottom-up wetland models in the GCP-CH_4 project (Saunois et al. 2024; Zhang et al. 2025). In total, 16 GCP-CH_4 models were studied, and models with similar process representations were merged. As a result, Table 2 summarizes 4 representative types of models.

From these models, we synthesized two key knowledge metrics: (1) direct and positive control of substrate availability on FCH_4; (2) Q10 (a measurable biogeochemistry parameter), as an essential metric to reflect how FCH_4 responds to temperature.

First, the GCP-CH_4 project's models used different variables as proxies of substrate availability, including soil labile carbon availability (C_{labile} by DLEM), net primary productivity (NPP by TEM), or soil heterotrophic respiration (RH by ELM), because direct estimates of substrate availability (e.g., acetate) are not made in current-generation large-scale wetland models. In practice, the utilization of these proxy variables was well supported by empirical knowledge. For example, higher NPP could increase root exudates and labile carbon inputs, thereby enhancing methanogenesis (Helfter et al. 2022; Zhou et al. 2021). Similarly, we used GPP as a proxy for NPP, since NPP is not available at EC sites, and importantly, GPP and NPP are highly related (Wang et al. 2025).

Second, Q10 represents the temperature sensitivity of FCH_4, which is quantified using the $(R2/R1)^{10/(T2-T1)}$. R2 and R1 are FCH_4 under warmed (T2) temperature versus control (T1) temperature. In practice, Q10 can be derived from observed flux-temperature relationships in field measurements or from manipulative warming experiments (Hu et al. 2026). Incorporating a realistic range of Q10 into the KGML framework during training could ensure biologically consistent responses of FCH_4 to temperature changes. Thus, we surveyed existing literature through Google Scholar using relevant keywords (wetland, CH_4, warming, Q10) for extratropical wetland ecosystems. Several studies directly reported Q10 values and were summarized in Table 3. By incorporating constraints from field observations and experimental manipulations, the KGML model can better account for temperature sensitivity, resulting in more biologically consistent reconstructions of multi-decadal FCH_4.

2.2.2 | Modeling Framework

The KGML framework has two stages: training and reconstruction (Figure 1). During the training stage, inputs to the KGML model included daily EC tower-based GPP, air temperature, precipitation, radiation, wind speed, humidity, and air pressure, as well as the 3/7/30-day moving means of air temperature and cumulative precipitation, and MODIS reflectance at EC sites. The output was the EC tower measured daily sum FCH_4.

We trained and tested one KGML model at each site, with 80%/20% randomly split data for testing. The loss function considered root mean square error (RMSE) and two knowledge constraint terms (Section 2.2.1): (1) positive control of substrate availability on FCH_4, so that the derivative of FCH_4 to GPP ($\partial FCH_4/\partial GPP$) is positive; (2) Q10 ranged from 1.4 to 5.8 (Table 3). While $\partial FCH_4/\partial GPP$ can be automatically provided by the neural network, Q10 estimation requires mathematical approximation. First, we used the Arrhenius equation to approximate FCH_4 (R):

$$R = \mathrm{A} \times \mathrm{e}^{-\mathrm{Ea}/\mathrm{kT}}$$

TABLE 2 | Key knowledge derived from representative process-based models in the GCP-CH_4 project (Saunois et al. 2024).

Model name	Governing equation (see footnote details)	Temperature response	Substrate control	References
DLM	$F = C_{labile} \times f(pH) \times f(T) - O$	$Q10^{(T-T0)/10}$	C_{labile}	Tian et al. (2011)
ELM	$F = RH \times f(pH) \times f(T) - O$	$Q10^{(T-T0)/10}$	RH	Riley et al. (2011)
LPJ-WSL	$F = RH \times r_{CH4:C} \times f_{ecosys}$	Through temperature-dependent $r_{CH4:C}$ and f_{ecosys} scaling terms	RH	Zhang et al. (2017)
TEM-MDM	$F = NPP \times f(pH) \times f(T) - O$	$Q10^{(T-T0)/10}$	NPP	Zhuang et al. (2004)

Abbreviations: C_{labile}, soil labile carbon pool; f_{ecosys}, scaling terms for each ecosystem type; NPP, net primary productivity; O, oxidation consumption rate of CH_4 within the soil column; $r_{CH4:C}$, ratio of CH_4 to CO_2 emissions; RH, soil heterotrophic respiration.

TABLE 3 | Independently measured Q10 for wetland FCH_4, compiled from the literature.

Site	Latitude	Longitude	Wetland type	Warm (°C)	Q10	References
Stordalen	68.35	18.82	Bog	4–24	1.9–5.8	Lupascu et al. (2012)
SPRUCE	48.98	−93.45	Bog	4.5	1.73–2.57	Gill et al. (2017)
BCMCA	27.68	80.7	Marsh	10–30	1.4–3.6	Inglett et al. (2012)
Shanyutan	26	119.57	Marsh	—	2.8–5.78	Wang et al. (2015)
Loch More	58.4	−3.7	Bog	5–15	2.2–3.0	MacDonald et al. (1998)
Aapa Mire	63.73	20.1	Fen	2–20	1.4–4.4	Bergman et al. (1998)
Copenhagen	55.8	12.57	Swamp	0–25	3.8–5.4	Westermann and Ahring (1987)

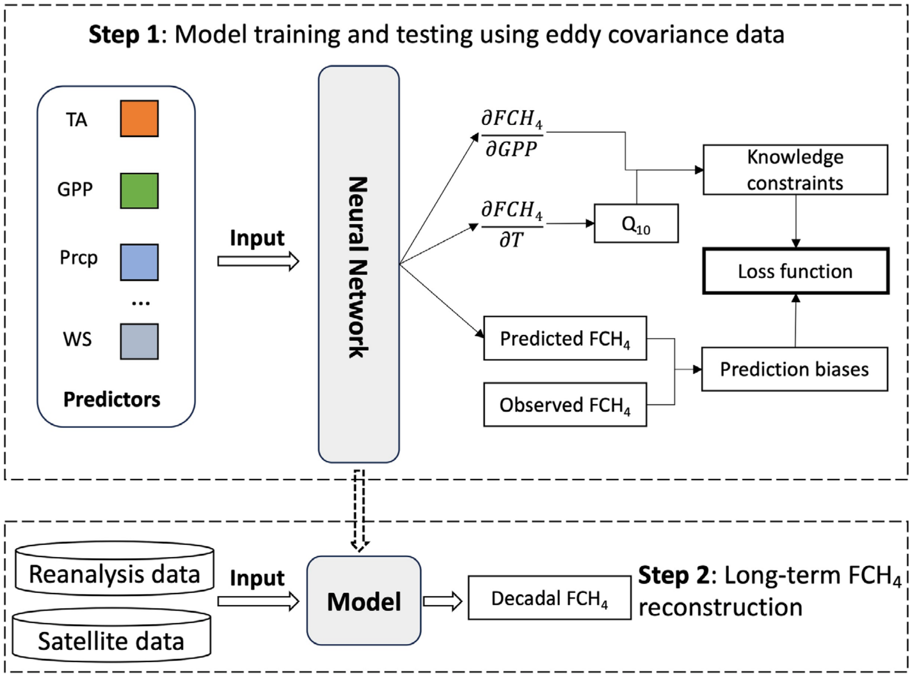

FIGURE 1 | Technical workflow of the Knowledge-Guided Machine Learning (KGML) reconstruction. The KGML framework involves a training stage using EC observations and meteorological and satellite inputs to learn FCH_4 emissions, guided by knowledge constraints (positive GPP influence and realistic temperature sensitivity). In the reconstruction stage, the trained models are applied to long-term satellite and reanalysis datasets (2000–2024) to generate daily wetland FCH_4 for analyzing trends, budgets, and environmental drivers across ecosystems.

where Ea is the activation energy, A is the pre-exponential rate constant, k is the Boltzmann constant, and T is the temperature. Taking the derivative of R to T, and replacing $A \times e^{-Ea/kT}$ by R gives:

$$dR/dT = A \times e^{-Ea/kT} \times Ea/kT^2$$

$$dR/dT = R \times Ea/kT^2$$

$$Ea/k = dR/dT/R \times T^2$$

Then, calculate Q10 by dividing R at 10 degree warming condition (R(T + 10)) by R at control condition (R(T)), and then replace Ea/k by $dR/dt/R \times T^2$:

$$R(T+10) = A \times e^{-Ea/k(T+10)}$$

$$R(T) = A \times e^{-Ea/kT}$$

$$Q10 = R(T+10)/R(T) = e^{Ea/k\ (1/T - 1/(T+10))}$$

$$Q10 = e^{dR/dT/R \times 10T/(T+10)} = e^{dFCH_4/dT/FCH_4 \times 10T/(T+10)}$$

Now, all terms within the Q10 approximation function (FCH_4, $dFCH_4/dT$, T) can automatically be provided by the neural network.

During the reconstruction stage, inputs to the KGML model included 2000 to 2024 GOSIFF-GPP (Li and Xiao 2019); ERA5 (Hersbach et al. 2020) air temperature, precipitation, radiation, wind speed, humidity, and air pressure; 3, 7, and 30-day moving averages of air temperature; and 3, 7, and 30-day cumulative precipitation. MODIS reflectance data were also used. The model's goal is to predict daily FCH_4 from 2000 to 2024. Such reconstructions provide a comprehensive, knowledge-constrained, and long-term record of wetland FCH_4 emissions across diverse ecosystems, enabling analysis of long-term budgets, trends, and their environmental controls.

3 | Results

3.1 | Reconstructed Wetland FCH_4 Budget

Training and testing the KGML model with EC FCH_4 data, along with knowledge constraints, yielded a very accurate model (Figure S1). For example, the coefficient of determination (R^2) ranged from 0.66 to 0.96 for the testing dataset. Note that the KGML model performed relatively worse at two sites due to some extreme data samples (abnormally high CH_4 emission observations at US-Los and US-Elm).

Additionally, we conducted temporal cross-validation by dividing the time series data into three continuous segments, reserving one-third for validation. This method allows us to effectively test the model's capability on unseen data, as the validation dataset comprises entirely different years compared to the training datasets. Our findings reveal that the model is robust across most sites, with testing R^2 values ranging from 0.5~0.92, compared to R^2 values of 0.66~0.96 observed with random sampling across all the sites. An exception was observed at the US-LA2 site, where the R^2 declined from 0.84 in the training phase to 0.26 in the test phase, indicating significant overfitting during temporal extrapolation. This decline can be attributed to the fact that 82% of daily data points during the observational period are missing. A significant data gap challenges the model's effectiveness. Therefore, we acknowledge that temporal cross-validation is a more stringent test of the model's ability to generalize across years and conditions not present in the training dataset. Overall, our results remain robust, with 10 out of 11 sites validating the major conclusions of our study.

Across all sites, substantial environmental changes occurred over the past two decades, as evidenced by the normalized mean annual temperature (MAT) showing significant increases (Figure 2). However, most of the EC tower data were only available during the recent decade (after 2015; Table 1; Figure 2), making it challenging to extrapolate the learned relationships between environmental drivers and FCH_4 back to the earlier decade, when environmental conditions differed substantially due to widespread warming and greening (Lian et al. 2022). Biogeochemical knowledge (Table 2) suggested that the colder climate and lower GPP during the past decade likely led to reduced FCH_4. By incorporating such knowledge constraints on how FCH_4 should respond to environmental changes, the KGML approach reduced the risk of misattributing the FCH_4-temperature-GPP relationship to other covariates, thereby enabling more robust reconstructions.

The reconstructed mean annual wetland FCH_4 budgets (Figure 3) ranged from 1.6 ± 0.1~$52.1 \pm 7.1\,gCH_4\ m^{-2}\,year^{-1}$ across the 11 sites. The highest emissions occurred at US-LA2, a sub-tropical freshwater marsh site, which was relatively warm (MAT ~16°C) and received the highest amount of rainfall (MAP ~1500 mm $year^{-1}$) across the sites (Table 1). Similarly, the lowest emissions occurred at the UC-ICs Arctic site, which had the coldest MAT (−9.2°C) and a short snow-free season. Variations exist at most sites due to different hyperparameters (configuration parameters) of the KGML reconstruction, and the percentage changes of annual budget (standard deviation divided by mean annual FCH_4) were as high as 19% (US-BZF subarctic fen site), indicating relatively large uncertainty.

3.2 | Reconstructed Wetland FCH_4 Trend

The reconstructed annual FCH_4 from 2000 to 2024 showed significant long-term trends at all four cold sites (US-BZB, US-BZF, US-ICs, US-NGB), whose MAT was below 0°C (Figure 4a). These four sites represented a wide range of wetland types, including

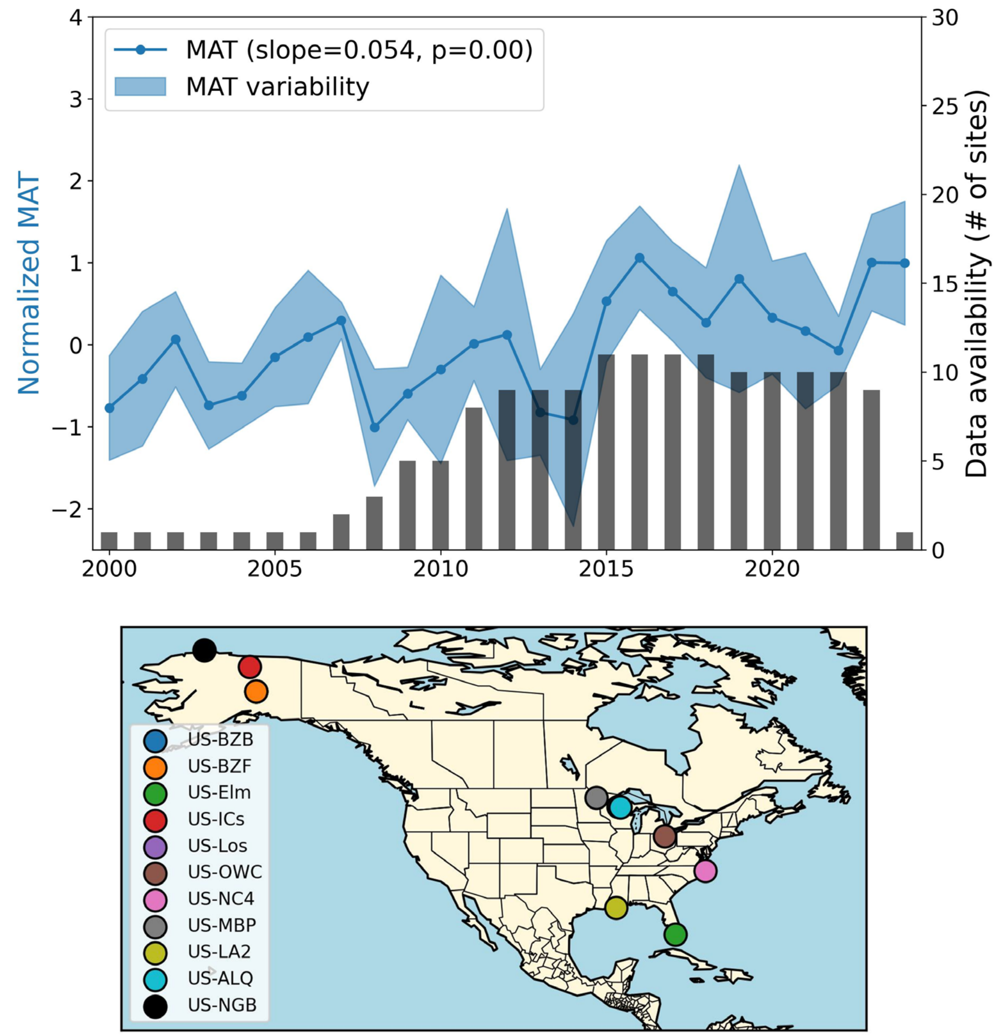

FIGURE 2 | The shift in mean annual temperature over the past two decades overlaps with the existence of the EC tower observational sites. The Inset Map is of EC site locations used in this study.

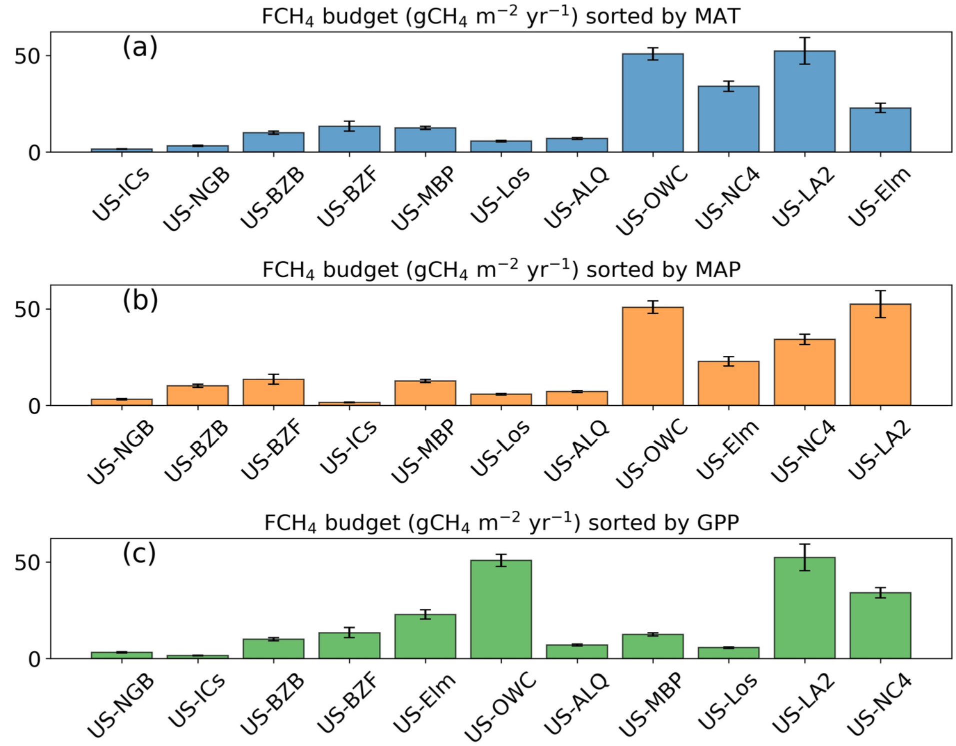

FIGURE 3 | Mean annual budget (2000–2024) of FCH_4 across all sites: (a) sorted by mean annual temperature (MAT); (b) sorted by mean annual precipitation (MAP); and (c) sorted by mean annual gross primary productivity (GPP). The error bars represent the uncertainties from the ensemble KGML reconstructions with the top 10 best-performing models.

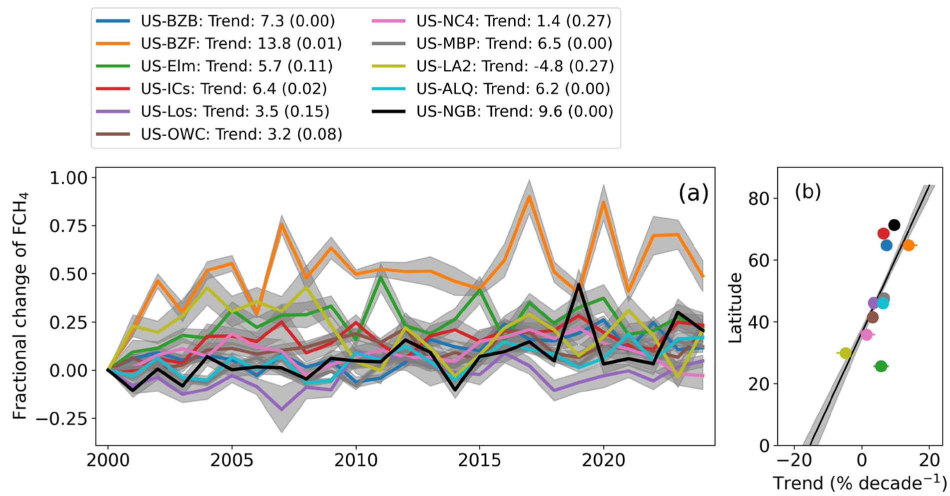

FIGURE 4 | (a) Fractional change in FCH_4, at the 11 EC sites. The legend includes the slope (unit % change per decade) and corresponding *p*-values in parentheses; the shaded area represents the uncertainties from the ensemble KGML reconstructions with the top 10 best-performing KGML models. (b) Relationship between reconstructed trends versus latitude.

thermokarst bog (US-BZB), fen over a thick layer of peat (US-BZF), and wet tundra sites (US-ICs, US-NGB). Their annual FCH_4 budgets increased by between 6.4% and 13.8% per decade, with the largest trend at the US-BZF site. This site differs markedly from other sub-Arctic sites, primarily in vegetation composition and hydrology. US-BZF is a rich fen in the Tanana River floodplain dominated by vascular species (e.g., Equisetum, Carex, and Potentilla), which facilitate the upward transport of CH_4 (Euskirchen et al. 2020). This site is also underlain by a thick peat layer (~1 m) (Thayamkottu et al. 2024) that provides abundant organic carbon substrates and therefore exhibits both the highest emission rate and decadal trend among the four cold sites.

Across relatively warmer sites (US-MBP, US-ALQ, US-Los), whose MATs were between 0°C and 10°C (Table 1), US-MBP and US-ALQ exhibited more moderate but statistically significant trends of 6%–7% changes per decade. However, US-Los showed a weaker trend (3.5% per decade) that was not statistically significant (*p*-value = 0.15). At the hottest sites, where MATs were between 10°C and 25°C, trends were all non-significant. Furthermore, the second-hottest but also the wettest site, US-LA2 (MAT 21°C, MAP 1452 mm), showed a statistically non-significant (p-value = 0.27) negative trend of −4.8% per decade.

Importantly, the decadal trends in FCH_4 correlated well with latitudes; specifically, the decadal trend significantly declined from high to low latitudes (Figure 4b). This correlation led to the hypothesis that relatively cold northern wetlands tended to respond more dramatically to environmental changes, regardless of the wetland type (i.e., bog, fen, wet tundra). However, we acknowledged that reconstructions at more EC sites are needed to provide further support for this hypothesis, given that only 11 sites were used to infer the latitudinal relationship.

3.3 | Comparison With Other Bottom-Up Estimates

The most recent GCP-CH_4 budget (Saunois et al. 2024) provided modeled bottom-up estimates of FCH_4 across global wetlands, serving as a scientific foundation for climate assessment and mitigation activities. As the largest natural source of FCH_4, accurate quantification of wetland FCH_4 has prominent impacts on climate policy. This study provided a critical long-term benchmark dataset of wetland FCH_4 at targeted locations. To compare, we first extracted the GCP-CH_4 grid-cell total emissions at the EC site locations and scaled them by GCP-CH_4 wetland inundation fraction to obtain the wetland CH_4 emission intensity (FCH_4: $gCH_4\ m^{-2}year^{-1}$).

We found that GCP-CH_4 overestimated FCH_4 at 10 out of 11 EC wetland sites (the exception was US-OWC) by between $9\,gCH_4\ m^{-2}year^{-1}$ (US-LA2) and $68\,gCH_4\ m^{-2}year^{-1}$ (US-Elm) (Figure 5). The overestimation of FCH_4 by GCP-CH_4 does not necessarily suggest overestimation of total wetland FCH_4 because the inundation area also plays a role (Bernard et al. 2025; Zhang et al. 2021), though this is out of the scope for this study. However, the overestimation by the GCP-CH_4 models suggests an urgent need to improve model parameterizations and reduce the discrepancy against EC observed FCH_4 (Ito et al. 2023; Zhang, Bansal, et al. 2023).

Similarly, we found a large mismatch in decadal trends estimated by GCP-CH_4 bottom-up models versus the KGML reconstructions. GCP-CH_4's estimates were overestimated in six out of 11 sites and underestimated in the other five sites, resulting in a much larger range of decadal trends in GCP-CH_4 estimates (−12% to 28% changes per decade). The overestimation and underestimation would likely cancel out when aggregating total CH_4 emissions over a large-scale region, which may explain why a limited long-term trend has been identified in GCP-CH_4's

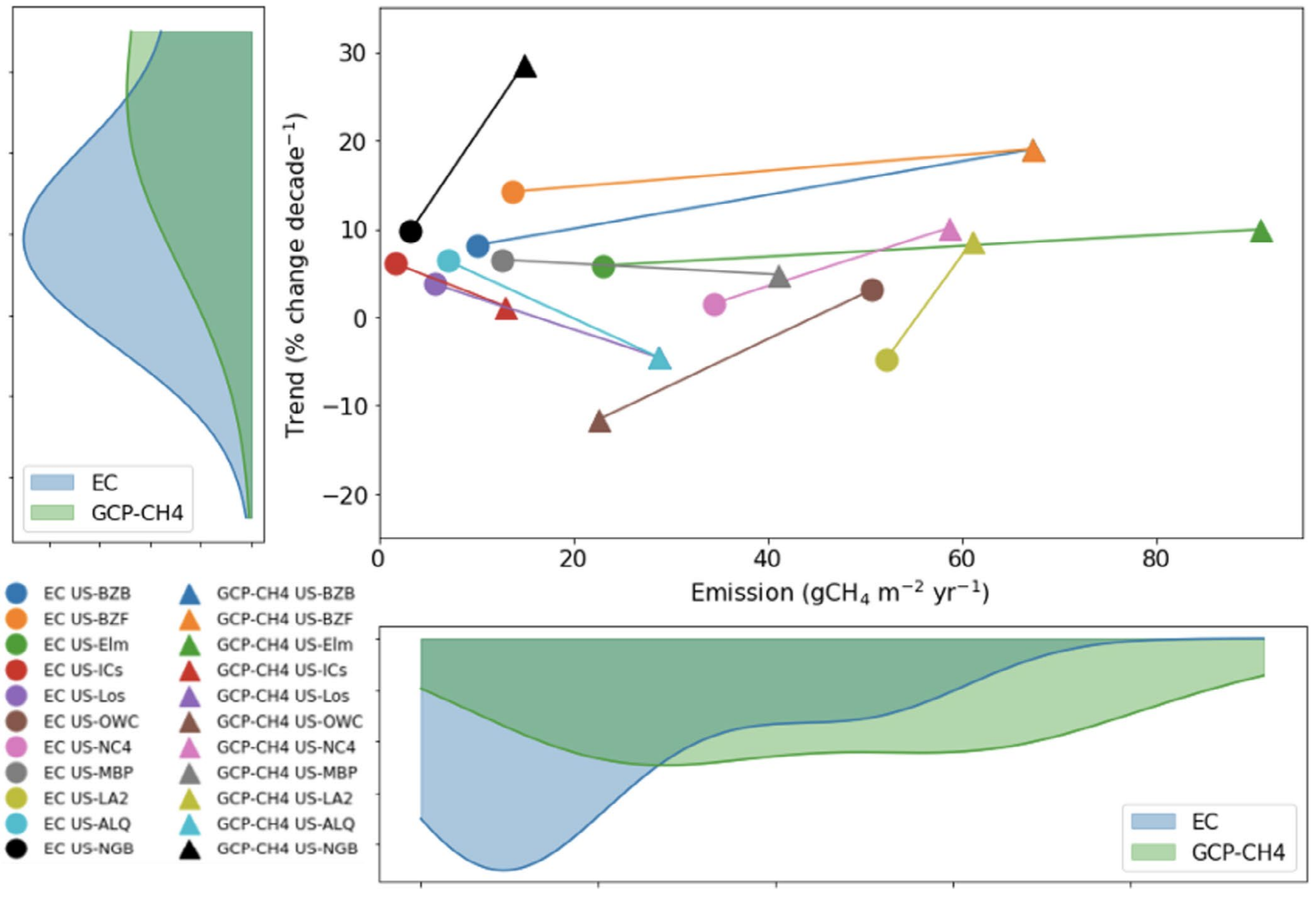

FIGURE 5 | Comparison between reconstructed EC FCH_4 (this study) and GCP-CH_4 FCH_4 (Saunois et al. 2024) at 11 sites. Linked symbols represent EC reconstruction and GCP-CH_4 bottom-up estimates for the same site.

estimates, for example, over the boreal Arctic region (Yuan et al. 2024).

3.4 | Attributions of the FCH_4 Trend

To quantify the contribution of different driving factors (i.e., temperature, water, vegetation, and other interactive effects), we conducted a step-wise attribution analysis. We sequentially removed the long-term trends and only used the repeated annual cycle of relevant variables for temperature (air temperature, 3/7/30-day moving average air temperature), water (precipitation, 3/7/30-day cumulative precipitation), and vegetation (GPP). The resultant changes in FCH_4 trends driven by detrended forcings inform the contributions of each factor to the decadal trend in FCH_4.

We found that temperature had a widespread positive contribution to the FCH_4 decadal trends (Figure 6), regardless of the climate zones or wetland types. Such responses were ensured by incorporating the Q10 temperature constraints during the training of the KGML model, thereby improving the robustness of the reconstruction not only for FCH_4 magnitude but, more importantly, for the functional response of FCH_4 to temperature.

The second widespread contributor was the interaction terms that could not be solely explained by temperature, water, or vegetation dynamics. The contributions from interactions comprised both the direct interactive effects (among temperature, water, and GPP) and indirect effects. The indirect effects were partly due to the limited number of input variables (predictor variables) used for the KGML model, which was necessary for the decadal reconstruction from 2000 to 2024. Many potential variables, such as water table depth and nutrient availability (Yazbeck et al. 2025; Yang et al. 2025), were not available across the sites. Therefore, when these variables may have played an important role in driving long-term trends in FCH_4 at specific sites, the KGML would attempt to represent this missing information by embedding known variables in a high-order nonlinear manner.

4 | Discussion

4.1 | Have Wetland FCH_4 Increased Over the Past Decades?

Evidence for observed multi-decadal and sustained changes in wetland FCH_4 is generally lacking in the literature, largely due to the short duration of eddy covariance (EC) records, which were mostly less than 8 years (Delwiche et al. 2021). In addition, observed FCH_4 at EC sites often shows strong interannual variability, making it difficult to isolate relatively small long-term trends (Knox et al. 2019). While ecosystem modeling and atmospheric inversion studies often suggest increasing CH_4 fluxes at the global scale (Peng et al. 2022), site-level observation-based evidence remains unclear. Previous efforts to reconstruct long-term FCH_4 at EC sites have applied gradient boosting decision trees (GBDT) to link site-specific drivers with FCH_4, yielding valuable insights (Feron et al. 2024). However, these reconstructions were limited by the short records from the FLUXNET-CH4 version 1 dataset. Also, GBDT's limited performance and weak extrapolation ability restricted its application for long-term reconstructions. For example, at two sites included in both Feron et al. (2024) and this study (US-NC4 and US-Los), the coefficients of determination (R^2) for testing datasets were substantially higher in this study (0.68 at US-Los, compared with 0.26 in Feron et al.; and 0.78 at US-NC4, compared with 0.53 in Feron et al.). Such differences in testing R^2 directly reflect how well models generalize to unobserved conditions.

This work addressed the short temporal coverage of FCH_4 measurements at EC sites by providing robust, multi-decadal reconstructions and assessments (Figure 4 ; Figure S2). We found consistent and significant increases in FCH_4 across northern cold wetland sites, providing compelling site-level evidence that cold wetlands might be experiencing strong positive interactions with environmental changes, regardless of differences in wetland type (bog, fen, wet tundra). By contrast, such increasing trends diminished or became non-significant at warmer, lower-latitude sites (e.g., US-LA2, US-Elm), suggesting that

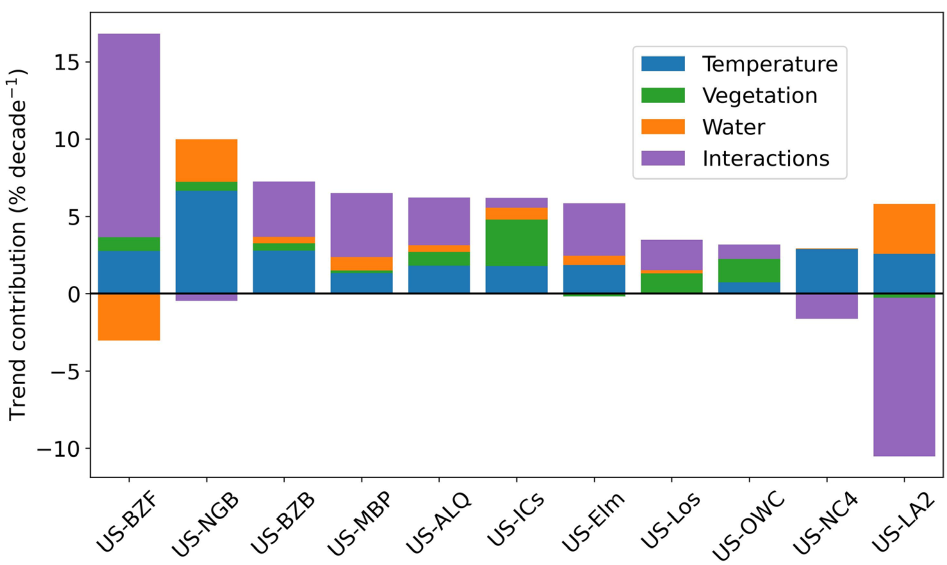

FIGURE 6 | Attribution of decadal changes of FCH_4 to temperature (air temperature, 3/7/30-day moving average air temperature), water (precipitation, 3/7/30-day cumulative precipitation), and vegetation (GPP). The interaction integrates unexplained drivers and other interactions.

FCH_4 sensitivity to climate warming is lower in warmer environments. These findings advance understanding of which wetland regions are most likely to drive long-term changes in the regional FCH_4 budget.

We note that this study quantifies wetland FCH_4 emission intensity (CH_4 emissions per unit wetland area). To quantify wetland contributions to the global atmospheric CH_4 budget, estimates of wetland inundation area (Bernard et al. 2025; Zhang et al. 2021) are required to scale FCH_4 to total emissions. However, large uncertainties in mapping global wetland inundation area and its long-term dynamics remain a major challenge (Zhang, Liu, et al. 2023), highlighting the urgent need for synergistic improvements in both research domains.

4.2 | How Do FCH_4 Emissions Budgets and Trends Differ Across Wetland Types?

This study covered five major wetland ecosystems: two wet tundra sites (US-ICs, US-NGB), one bog (US-BZB), four fens (US-BZF, US-MBP, US-Los, US-ALQ), three marshes (US-OWC, US-LA2, US-Elm), and one swamp (US-NC4). These ecosystems are fundamentally different in hydrology, nutrient availability, vegetation composition, soil carbon density, and other characteristics (Zedler and Kercher 2005). Below, we evaluate wetland-type-specific hypotheses using the reconstructed FCH_4 budgets and trends across wetland types.

First, we hypothesized that fens exhibit stronger long-term FCH_4 trends than bogs because their groundwater-fed hydrology sustains greater plant productivity and thus greater substrate availability. Fens also typically have higher and more stable water tables and thus more stable anaerobic conditions compared with nutrient-poor, rain-fed bogs. We examined a paired bog-fen comparison (US-BZB versus US-BZF), where climate conditions are similar (Table 1), since comparing US-BZB with fen sites in much warmer environments (US-MBP, US-ALQ, US-Los) is not informative. We found that US-BZF (fen) exhibited significantly higher annual FCH_4 (Figure 3) and decadal trends (Figure 4) than US-BZB (bog), thus supporting this hypothesis. Although nutrient availability and water tables were not explicitly included in the KGML model as predictors, the distinctions in nutrient and hydrological conditions at the two sites were likely encoded indirectly by using combinations of other available input variables from KGML's learned patterns.

Second, we hypothesized that marshes and swamps operate near optimal conditions (e.g., temperature, hydrology, substrate availability), such that further environmental changes (e.g., warming, greening, wetting) have only marginal impacts on FCH_4, compared with high-latitude tundra, bog, and fen wetlands. Our results supported this hypothesis, showing that marsh and swamp sites exhibited significantly higher annual FCH_4 emissions than bog, fen, and wet tundra sites (Figure 3). Furthermore, none of the marsh and swamp sites showed statistically significant long-term trends (Figure 4). We note, however, that this pattern does not necessarily imply a limited contribution of FCH_4 from marsh and swamp wetlands to regional and global budgets, since total emissions are the product of FCH_4 and wetland inundation area. The latter could substantially change due to regional wetting or drying (Lu et al. 2024).

4.3 | Has FCH_4 Exhibited Long-Term Seasonal Shifts?

To better understand the long-term seasonal changes in wetland FCH_4 and how they contribute to the trend in annual FCH_4, we grouped the daily FCH_4 into summer months (June, July, August) and fall months (September, October, November) and quantified the decadal trends for each season (Figure S3).

All high latitude bogs and fens sites (US-BZB, US-BZF, US-ICs, US-NGB) maintained similar or higher decadal trends in summer months compared with all seasons. With the US-BZF fen site being the most prominent site. Its FCH_4 trend increased from 14% (annual) to 19% (summer-only) per decade, suggesting this high-emission fen site experienced the shift of annual emissions towards summer months. Furthermore, no significant trend was detected during fall months for US-BZF, further supporting this point. This suggests that the window of FCH_4 at US-BZF is increasingly concentrated in the summer season, when warming, sustained water tables, and maximum plant productivity coincide to create optimal conditions for microbial methanogenesis and transport.

At warmer fen, marsh, and swamp sites (US-OWC, US-Los, US-Elm, US-NC4, US-LA2), where all-seasons decadal trends in FCH_4 were not statistically significant, their summer months still did not show significant decadal trends. However, a few sites showed significant decadal increases during fall months. For example, the US-Elm and US-OWC sites both showed about a 10%–11% increase in FCH_4 per decade during fall months only. This pattern suggests that at warmer sites during the summer season, microbial activity and plant-mediated transport might be near saturation, thereby limiting further sensitivity to environmental and vegetation changes. In contrast, the pronounced fall increase at US-OWC and US-Elm sites suggests that off-peak FCH_4 in the fall months has become more favorable for methane production and plant-mediated release.

4.4 | Traditional ML Versus KGML

If we remove the knowledge constraints and conduct the same training, testing, and reconstruction, how would such a pure ML approach compare to KGML? The comparative performance of the pure ML and KGML models demonstrates the superiority of KGML in both interpolation and extrapolation capabilities.

When the datasets were randomly sampled, the pure ML model achieved a training R^2 of 0.75 ± 0.2 and a testing R^2 of 0.65 ± 0.2, while the KGML model outperformed it with a training R^2 of 0.86 ± 0.1 and a testing R^2 of 0.75 ± 0.1, highlighting KGML's superiority in interpolation. When selecting datasets sequentially for testing, the pure ML model's performance dropped significantly, reaching a training R^2 of 0.46 ± 0.3 and a testing R^2 of 0.25 ± 0.6, compared to KGML's training R^2 of 0.73 ± 0.1 and testing R^2 of 0.60 ± 0.2, indicating KGML's better extrapolation capabilities as well.

Additionally, an examination of temperature response functions showed a more stable response learned by the KGML model. For example, at the US-BZB site, where both pure ML and KGML models achieved a testing accuracy of $R^2 = 0.82$. However, the pure ML model had an unstable temperature response, either declining then rising, with substantial uncertainty at lower temperatures. In contrast, the KGML model had a stable and reliable positive response function to temperature, demonstrating enhanced robustness.

Although KGML does not explicitly resolve each individual biogeochemical process of the target system, its knowledge-guided architecture and loss functions constrain the model to learn relationships that are consistent with established process understanding (Liu et al. 2024). Specifically for wetland CH_4 emissions, although the model is trained on eddy covariance FCH_4 measurements that represent the net balance of methane production, oxidation, and transport processes, KGML enables the model to implicitly learn process-consistent representations of these latent components. For example, the temperature sensitivity learned by the model reflects the combined temperature dependence of microbial methanogenesis and methanotrophic oxidation. In addition, both methanogenesis and methanotroph are strongly regulated by soil water availability. Therefore, variability in the model's temperature sensitivity under fluctuating hydrological conditions (e.g., precipitation and soil inundation) and shifts in anaerobic conditions could inform changes in methane transport pathways, including episodic ebullition and plant-mediated transport (Le Mer and Roger 2001).

4.5 | Limitations and Future Directions

A critical limitation of our analysis is the lack of EC sites with continuous records spanning the study period (2000–2024), which prevents rigorous validation of the reconstructed FCH_4 trends. While the integration of warming experiment data to infer Q10 values and the use of knowledge-based constraints improve the model's ability to extrapolate beyond the observational period (Liu et al. 2024; Yuan et al. 2022), direct validation against long-term flux records is needed.

Another limitation arises from the uncertainties and scale discrepancies between environmental forcings and EC flux measurements. For example, ERA5 reanalysis climate variables, GOSIF gross primary productivity, and MODIS reflectance products used in this study all operate at different spatial resolutions and temporal aggregations than EC tower footprints. These mismatches introduce additional uncertainty into both the model training and the reconstructed fluxes, particularly in heterogeneous landscapes where small-scale processes may not be well captured by coarse-scale forcing data. Future work should focus on the robust downscaling of coarse-resolution datasets (e.g., ERA5 forcings) and the improvement of harmonization between environmental datasets and wetland FCH_4 observations.

This study relies on 11 AmeriFlux sites, thus limiting the generality of our findings. Expanding the network to include more sites is critically important, particularly in underrepresented regions (Malone et al. 2022; Pallandt et al. 2024). The ongoing synthesis of FLUXNET-CH_4 (version 2) will provide unprecedented opportunities to improve the understanding of wetland FCH_4 across a much wider range of wetland ecosystems. For example, tropical wetlands are known to be major CH_4 sources (Chang et al. 2023; Murguia-Flores et al. 2023), but are not represented in this study. Incorporating EC data from tropical wetland systems will be essential to provide insights into long-term global wetland FCH_4 dynamics (Zhu et al. 2024).

We acknowledge that changes in plant community composition represent an important source of uncertainty in long-term wetland FCH_4 reconstructions. Although our analysis using NDVI suggests general system stability over time, NDVI does not fully capture shifts in species identity. Previous studies have shown that methane flux can vary significantly among different plant communities due to differences in vegetation biomass and functional characteristics that are not resolved by vegetation indices (Järvi-Laturi et al. 2025).

Moreover, wetland plant species can differ in their influence on methane production, oxidation, and transport (Goud et al. 2017; Määttä and Malhotra 2024). For example, species with aerenchymatous tissue can facilitate greater methane transport than species without aerenchyma. Because NDVI primarily reflects overall vegetation "greenness" rather than trait-based differences such as aerenchyma, using NDVI as a predictor could overlook species compositional shifts that alter methane emission pathways. Nevertheless, we included MODIS surface reflectance in model predictors, which provided compounded information on the plant traits that could reflect the spectral change due to the changes in the structure and composition of vegetation. Future work could incorporate species-level or functional trait datasets, as well as emerging remote sensing products capable of distinguishing wetland vegetation composition, to improve the long-term wetland FCH_4 reconstructions.

4.6 | Implications for Targeted Interventions and Sustainable Land Management Solutions

This study tackled critical challenges in characterizing trends in CH_4 emissions within wetland ecosystems, which exhibited varying sensitivities to unidentified drivers (Figure 6). Aside from differences in climate and vegetation, between-site variation in the size and effect of interactions likely resulted from factors previously shown to influence ecosystem structure and function, such as nutrient levels, water quality, lateral fluxes, and disturbances. The variation in unexplained interactions may also have important implications for resource management strategies that support nature-based solutions (Keesstra et al. 2018), as wetlands often provide a multitude of ecosystem services of significant economic and environmental value. The capacity of wetlands to capture and sequester carbon for extended time periods is particularly relevant (Were et al. 2019). Due to concerns about the positive feedback of wetland FCH_4 to global change (Zhang et al. 2017), studying wetlands where FCH_4 have reached saturation or where water management can be used as a tool for mitigation is important. To enhance existing models and data, it is essential to integrate landscape position, disturbances, and resource management activities in the development of high-resolution emission models. This work highlights the need for advancements in measurement infrastructure that will enable the design of targeted interventions and facilitate the practical assessment of wetland conservation and restoration efforts.

5 | Conclusions

In this study, we developed and applied a novel Knowledge-Guided Machine Learning (KGML) framework that integrated eddy-covariance (EC) flux measurements with key biogeochemical knowledge, such as the Q10 temperature sensitivity. We addressed the critical temporal limitation of EC flux measurements by reconstructing FCH_4 from 2000 to 2024 across 11 diverse wetland sites and revealed a significant decadal increase in annual FCH_4 at high-latitude sites (6% to 14% increase per decade), a trend that diminished sharply moving toward warmer, lower-latitude sites. Therefore, the results underscored the fact that northern wetlands have been highly sensitive to environmental change and pose a potentially positive feedback to the climate system. Attribution analysis further confirmed that temperature was the most widespread positive contributor to the observed decadal FCH_4 trends. The prominent interaction terms were identified as proxies for unaccounted interactions and unused environmental drivers, such as water table dynamics and complex soil characteristics, whose effects the non-linear KGML framework captures. Additionally, our reconstructed long-term FCH_4 time series can serve as a benchmark dataset for bottom-up biogeochemistry models. Compared with the GCP-CH_4 bottom-up model estimates, we found a persistent overestimation of FCH_4 magnitude and poor correspondence for long-term trends, indicating the need to improve model parameterizations related to FCH_4 and its responses to changes in environmental conditions to aid the development of effective mitigation strategies.

Author Contributions

Qing Zhu: conceptualization, formal analysis, methodology, resources, software, validation, visualization, writing – original draft. **Kyle A. Arndt:** conceptualization, data curation, validation, writing – review and editing. **Kunxiaojia Yuan:** data curation, software, validation, writing – review and editing. **Fa Li:** data curation, validation, visualization, writing – review and editing. **Qing Ying:** data curation, validation, writing – review and editing. **Licheng Liu:** funding acquisition, validation, writing – review and editing. **Eric Ward:** data curation, validation, writing – review and editing. **Avni Malhotra:** data curation, validation, writing – review and editing. **Jianqiu Zheng:** data curation, validation, writing – review and editing. **Fenghui Yuan:** data curation, validation, writing – review and editing. **Sparkle L. Malone:** funding acquisition, validation, writing – review and editing. **Gavin McNicol:** funding acquisition, validation, writing – review and editing. **Sara H. Knox:** validation, writing – review and editing. **William J. Riley:** supervision, writing – review and editing. **Margaret S. Torn:** supervision, writing – review and editing. **Shuo Chen:** validation, writing – review and editing. **Ben Riddell-Young:** validation, writing – review and editing. **Youmi Oh:** funding acquisition, validation, writing – review and editing. **Lori Bruhwiler:** conceptualization, validation, writing – review and editing.

Acknowledgements

This work was conducted as a part of the Synthesis Working Group funded by the National Science Foundation under grant #2153040, through the ESIIL, Colorado University Boulder. Q.Z. from Lawrence Berkeley National Laboratory (LBNL) is managed by the University of California for the U.S. Department of Energy under contract DE-AC02-05CH11231. We also acknowledge the use of AmeriFlux data resources provided by the U.S. Department of Energy's Office of Science. K.A.A. is supported with funding catalyzed by the TED Audacious Project (Permafrost Pathways). A.M. was supported by an Early Career Award from the U.S. Department of Energy, Office of Science, Biological and Environmental Research. F.L. acknowledges support from startup funds provided by The University of Texas at Austin.

Conflicts of Interest

The authors declare no conflicts of interest.

Data Availability Statement

Eddy covariance data (FCH_4, GPP, temperature, precipitation, solar radiation, wind speed, air pressure): https://ameriflux.lbl.gov/. MODIS Nadir BRDF-Adjusted Reflectance Daily data (MCD43A4): https://ladsweb.modaps.eosdis.nasa.gov/missions-and-measurements/products/MCD43A4. ERA5 forcing data (temperature, precipitation, solar radiation, wind speed, air pressure): https://cds.climate.copernicus.eu/datasets/derived-era5-single-levels-daily-statistics?tab=download. GOSIF-GPP: https://globalecology.unh.edu/data/GOSIF-GPP.html. Codes and reconstructed eddy covariance data: https://doi.org/10.5281/zenodo.19543891.

References

Baldocchi, D. 2014. "Measuring Fluxes of Trace Gases and Energy Between Ecosystems and the Atmosphere–the State and Future of the Eddy Covariance Method." *Global Change Biology* 20, no. 12: 3600–3609.

Bergman, I., B. H. Svensson, and M. Nilsson. 1998. "Regulation of Methane Production in a Swedish Acid Mire by pH, Temperature and Substrate." *Soil Biology and Biochemistry* 30, no. 6: 729–741.

Bernard, J., C. Prigent, C. Jimenez, et al. 2025. "The GIEMS-MethaneCentric Database: A Dynamic and Comprehensive Global Product of Methane-Emitting Aquatic Areas." *Earth System Science Data* 17, no. 6: 2985–3008. https://doi.org/10.5194/essd-17-2985-2025.

Beucler, T., P. Gentine, J. Yuval, et al. 2024. "Climate-Invariant Machine Learning." *Science Advances* 10, no. 6: eadj7250.

Bohrer, G., and S. McMurray. 2025. "AmeriFlux BASE US-OWC Old Woman." Creek (Version Ver. 6-5) [Data set]. AmeriFlux AMP, (Dataset). https://doi.org/10.17190/AMF/1418679.

Chang, K.-Y., W. J. Riley, N. Collier, et al. 2023. "Observational Constraints Reduce Model Spread but Not Uncertainty in Global Wetland Methane Emission Estimates." *Global Change Biology* 29, no. 15: 4298–4312.

Chen, S., K. Yuan, F. Li, Q. Zhu, and Q. Zhuang. 2025. "Hysteretic Temperature Sensitivity in Wetland CH_4 Emission Modeling." *Agricultural and Forest Meteorology* 372: 110704.

Chinta, S., X. Gao, and Q. Zhu. 2024. "Machine Learning Driven Sensitivity Analysis of E3SM Land Model Parameters for Wetland Methane Emissions." *Journal of Advances in Modeling Earth Systems* 16, no. 7: e2023MS004115.

Ciais, P., Y. Zhu, Y. Cai, et al. 2026. "Why Methane Surged in the Atmosphere During the Early 2020s." *Science* 391, no. 6785: eadx8262. https://doi.org/10.1126/science.adx8262.

Delwiche, K. B., S. H. Knox, A. Malhotra, et al. 2021. "FLUXNET-CH_4: A Global, Multi-Ecosystem Dataset and Analysis of Methane Seasonality From Freshwater Wetlands." *Earth System Science Data Discussions* 2021: 1–111.

Desai, A. 2025. "AmeriFlux BASE US-Los Lost Creek." (Version Ver. 33-5) [Data set]. AmeriFlux AMP, (Dataset). https://doi.org/10.17190/AMF/1246071.

Euskirchen, E. 2025a. "AmeriFlux BASE US-BZB Bonanza Creek Thermokarst Bog." (Version Ver. 5-5) [Data set]. AmeriFlux AMP, (Dataset). https://doi.org/10.17190/AMF/1773401.

Euskirchen, E. 2025b. "AmeriFlux BASE US-BZF Bonanza Creek Rich Fen." (Version Ver. 5-5) [Data set]. AmeriFlux AMP, (Dataset). https://doi.org/10.17190/AMF/1756433.

Euskirchen, E., G. Shaver, and S. Bret-Harte. 2025. "AmeriFlux BASE US-ICs Imnavait Creek Watershed Wet Sedge Tundra." (Version Ver. 11-5) [Data set]. AmeriFlux AMP, (Dataset). https://doi.org/10.17190/AMF/1246130.

Euskirchen, E. S., E. S. Kane, C. W. Edgar, and M. R. Turetsky. 2020. "When the Source of Flooding Matters: Divergent Responses in Carbon Fluxes in an Alaskan Rich Fen to Two Types of Inundation." *Ecosystems* 23, no. 6: 1138–1153.

Feron, S., A. Malhotra, S. Bansal, et al. 2024. "Recent Increases in Annual, Seasonal, and Extreme Methane Fluxes Driven by Changes in Climate and Vegetation in Boreal and Temperate Wetland Ecosystems." *Global Change Biology* 30, no. 1: e17131.

Gill, A. L., M.-A. Giasson, R. Yu, and A. C. Finzi. 2017. "Deep Peat Warming Increases Surface Methane and Carbon Dioxide Emissions in a Black Spruce-Dominated Ombrotrophic Bog." *Global Change Biology* 23, no. 12: 5398–5411.

Goud, E. M., T. R. Moore, and N. T. Roulet. 2017. "Predicting Peatland Carbon Fluxes from Non-Destructive Plant Traits." *Functional Ecology* 31, no. 9: 1824–1833.

Helfter, C., M. Gondwe, M. Murray-Hudson, et al. 2022. "Phenology Is the Dominant Control of Methane Emissions in a Tropical Non-Forested Wetland." *Nature Communications* 13, no. 1: 133.

Hersbach, H., B. Bell, P. Berrisford, et al. 2020. "The ERA5 Global Reanalysis." *Quarterly Journal of the Royal Meteorological Society* 146, no. 730: 1999–2049.

Hu, H., K. Xue, Y. Sun, et al. 2026. "Reducing the Discrepancy in Quantifying the Temperature Dependence of Global Wetland Methane Emission." *Global Change Biology* 32, no. 2: e70748. https://doi.org/10.1111/gcb.70748.

Inglett, K. S., P. W. Inglett, K. R. Reddy, and T. Z. Osborne. 2012. "Temperature Sensitivity of Greenhouse Gas Production in Wetland Soils of Different Vegetation." *Biogeochemistry* 108, no. 1: 77–90.

Ito, A., T. Li, Z. Qin, et al. 2023. "Cold-Season Methane Fluxes Simulated by GCP-CH_4 Models." *Geophysical Research Letters* 50, no. 14: e2023GL103037.

Järvi-Laturi, E., T. Tahvanainen, E. Koskinen, et al. 2025. "Plant Community Composition Controls Spatial Variation in Year-Round Methane Fluxes in a Boreal Rich Fen." *EGUsphere* 2025: 1–36.

Jian, J., M. K. Steele, L. Zhang, et al. 2022. "On the Use of Air Temperature and Precipitation as Surrogate Predictors in Soil Respiration Modelling." *European Journal of Soil Science* 73, no. 1: e13149.

Jin, Z., L. Liu, Q. Yang, et al. 2026. "Knowledge-Guided Machine Learning for Global Change Ecology Research." *Global Change Biology* 32: e70742. https://doi.org/10.1111/gcb.70742.

Keesstra, S., J. Nunes, A. Novara, et al. 2018. "The Superior Effect of Nature Based Solutions in Land Management for Enhancing Ecosystem Services." *Science of the Total Environment* 610: 997–1009.

Knox, S. H., S. Bansal, G. McNicol, et al. 2021. "Identifying Dominant Environmental Predictors of Freshwater Wetland Methane Fluxes Across Diurnal to Seasonal Time Scales." *Global Change Biology* 27, no. 15: 3582–3604.

Knox, S. H., R. B. Jackson, B. Poulter, et al. 2019. "FLUXNET-CH 4 Synthesis Activity: Objectives, Observations, and Future Directions." *Bulletin of the American Meteorological Society* 100, no. 12: 2607–2632.

Le Mer, J., and P. Roger. 2001. "Production, Oxidation, Emission and Consumption of Methane by Soils: A Review." *European Journal of Soil Biology* 37, no. 1: 25–50.

Li, X., and J. Xiao. 2019. "Mapping Photosynthesis Solely From Solar-Induced Chlorophyll Fluorescence: A Global, Fine-Resolution Dataset of Gross Primary Production Derived From OCO-2." 11: 2563. https://doi.org/10.3390/rs11212563.

Lian, X., S. Jeong, C.-E. Park, et al. 2022. "Biophysical Impacts of Northern Vegetation Changes on Seasonal Warming Patterns." *Nature Communications* 13, no. 1: 3925. https://doi.org/10.1038/s41467-022-31671-z.

Liu, L., W. Zhou, K. Guan, et al. 2024. "Knowledge-Guided Machine Learning Can Improve Carbon Cycle Quantification in Agroecosystems." *Nature Communications* 15, no. 1: 357.

Lu, D., Y. Zheng, X. Liu, and J. Chang. 2024. "Changes in Wetland Landscape and Inundation Patterns in the Middle and Lower Reaches of the Yangtze River Basin From 1990 to 2020." *Ecological Indicators* 161: 111992.

Lupascu, M., J. L. Wadham, E. R. Hornibrook, and R. D. Pancost. 2012. "Temperature Sensitivity of Methane Production in the Permafrost Active Layer at Stordalen, Sweden: A Comparison With Non-Permafrost Northern Wetlands." *Arctic, Antarctic, and Alpine Research* 44, no. 4: 469–482.

Ma, S., I. F. Creed, and P. Badiou. 2024. "New Perspectives on Temperate Inland Wetlands as Natural Climate Solutions Under Different CO_2-Equivalent Metrics." *NPJ Climate and Atmospheric Science* 7, no. 1: 222. https://doi.org/10.1038/s41612-024-00778-z.

Määttä, T., and A. Malhotra. 2024. "The Hidden Roots of Wetland Methane Emissions." *Global Change Biology* 30, no. 2: e17127.

MacDonald, J. A., D. Fowler, K. J. Hargreaves, U. Skiba, I. D. Leith, and M. B. Murray. 1998. "Methane Emission Rates From a Northern Wetland; Response to Temperature, Water Table and Transport." *Atmospheric Environment* 32, no. 19: 3219–3227.

Malone, S. L., Y. Oh, K. A. Arndt, et al. 2022. "Gaps in Network Infrastructure Limit Our Understanding of Biogenic Methane Emissions for the United States." *Biogeosciences* 19: 2507–2522. https://doi.org/10.5194/bg-19-2507-2022.

McNicol, G., E. Fluet-Chouinard, Z. Ouyang, et al. 2023. "Upscaling Wetland Methane Emissions From the FLUXNET-CH_4 Eddy Covariance Network (UpCH$_4$ v1. 0): Model Development, Network Assessment, and Budget Comparison." *AGU Advances* 4, no. 5: e2023AV000956.

Murguia-Flores, F., V. J. Jaramillo, and A. Gallego-Sala. 2023. "Assessing Methane Emissions From Tropical Wetlands: Uncertainties From Natural Variability and Drivers at the Global Scale." *Global Biogeochemical Cycles* 37, no. 9: e2022GB007601. https://doi.org/10.1029/2022GB007601.

Nisbet, E. G., M. R. Manning, E. J. Dlugokencky, et al. 2019. "Very Strong Atmospheric Methane Growth in the 4 Years 2014–2017: Implications for the Paris Agreement." *Global Biogeochemical Cycles* 33, no. 3: 318–342.

Noormets, A., J. King, B. Mitra, G. Miao, and M. Aguilos. 2024. "AmeriFlux FLUXNET-1F US-NC4 NC_AlligatorRiver." (Version Ver. 4-6, AmeriFlux AMP (Dataset)) [Data set]. https://doi.org/10.17190/AMF/1902837.

Olson, B. 2025. "AmeriFlux BASE US-ALQ Allequash Creek Site." (Version Ver. 22-5) [Data set]. AmeriFlux AMP, (Dataset). https://doi.org/10.17190/AMF/1480323.

Pallandt, M. M., M. Jung, K. Arndt, et al. 2024. "High-Latitude Eddy Covariance Temporal Network Design and Optimization." *Journal of Geophysical Research: Biogeosciences* 129, no. 10: e2024JG008406.

Peng, S., X. Lin, R. L. Thompson, et al. 2022. "Wetland Emission and Atmospheric Sink Changes Explain Methane Growth in 2020." *Nature* 612, no. 7940: 477–482.

Riley, W. J., Z. M. Subin, D. M. Lawrence, et al. 2011. "Barriers to Predicting Changes in Global Terrestrial Methane Fluxes: Analyses Using CLM4Me, a Methane Biogeochemistry Model Integrated in CESM." *Biogeosciences* 8, no. 7: 1925–1953.

Roman, T., A. Hill, R. Kolka, T. Griffis, and J. Deventer. 2025. "AmeriFlux BASE US-MBP Marcell Bog Lake Peatland." (Version Ver. 5-5) [Data set]. AmeriFlux AMP, (Dataset). https://doi.org/10.17190/AMF/1767835.

Saunois, M., A. Martinez, B. Poulter, et al. 2024. "Global Methane Budget 2000–2020." *Earth System Science Data* 17, no. 5: 1873–1958.

Saunois, M., A. R. Stavert, B. Poulter, et al. 2020. "The Global Methane Budget 2000–2017." *Earth System Science Data* 12: 1561–1623. https://doi.org/10.5194/essd-12-1561-2020.

Schuster, L., P. Taillardat, P. I. Macreadie, and M. E. Malerba. 2024. "Freshwater Wetland Restoration and Conservation Are Long-Term Natural Climate Solutions." *Science of the Total Environment* 922: 171218. https://doi.org/10.1016/j.scitotenv.2024.171218.

Starr, G., and S. Oberbauer. 2025. "AmeriFlux BASE US-Elm Everglades (Long Hydroperiod Marsh)." (Version Ver. 7-5) [Data set]. AmeriFlux AMP, (Dataset). https://doi.org/10.17190/AMF/1246118.

Thayamkottu, S., T. L. Smallman, J. Pärn, Ü. Mander, E. S. Euskirchen, and E. S. Kane. 2024. "Greening of a Boreal Rich Fen Driven by CO2 Fertilisation." *Agricultural and Forest Meteorology* 359: 110261.

Tian, H., X. Xu, C. Lu, et al. 2011. "Net Exchanges of CO_2, CH_4, and N_2O Between China's Terrestrial Ecosystems and the Atmosphere and Their Contributions to Global Climate Warming." *Journal of Geophysical Research: Biogeosciences* 116, no. G2: G02011.

Torn, M., and S. Dengel. 2023. "AmeriFlux BASE US-NGB NGEE Arctic Barrow." (Version Ver. 5-5) [Data set]. AmeriFlux AMP. https://doi.org/10.17190/AMF/1436326.

Wang, C., D. Y. Lai, C. Tong, W. Wang, J. Huang, and C. Zeng. 2015. "Variations in Temperature Sensitivity (Q 10) of CH_4 Emission From a Subtropical Estuarine Marsh in Southeast China." *PLoS One* 10, no. 5: e0125227.

Wang, X., X. Qiao, S. Lin, et al. 2025. "Scale-Dependent Variations in Photosynthetic Processes Mediate Net Primary Productivity in Temperate Forests." *Forest Ecosystems* 14: 100366.

Wang, Z., C. B. Schaaf, Q. Sun, Y. Shuai, and M. O. Román. 2018. "Capturing Rapid Land Surface Dynamics With Collection V006 MODIS BRDF/NBAR/Albedo (MCD43) Products." *Remote Sensing of Environment* 207: 50–64. https://doi.org/10.1016/j.rse.2018.02.001.

Ward, E., S. Merino, C. Stagg, and K. Krauss. 2025. "AmeriFlux BASE US-LA2 Salvador WMA Freshwater Marsh." (Version Ver. 4-5) [Data set]. AmeriFlux AMP (Dataset). https://doi.org/10.17190/AMF/1543387.

Watts, J. D., E. Ordway, S. L. Malone, et al. 2026. "A Global Methane Observation System to Track Climate Feedbacks for Verifiable Climate Impact." *Science* 391, no. 6792: 1324–1327.

Were, D., F. Kansiime, T. Fetahi, A. Cooper, and C. Jjuuko. 2019. "Carbon Sequestration by Wetlands: A Critical Review of Enhancement Measures for Climate Change Mitigation: D. Were Et al." *Earth Systems and Environment* 3, no. 2: 327–340.

Westermann, P., and B. K. r. Ahring. 1987. "Dynamics of Methane Production, Sulfate Reduction, and Denitrification in a Permanently Waterlogged Alder Swamp." *Applied and Environmental Microbiology* 53, no. 10: 2554–2559.

Yang, S., J. Tang, L. Zhen, et al. 2025. "Unraveling the Depth-Dependent Causal Dynamics of Methanogenesis and Methanotrophy in a High-Latitude Fen Peatland." *Environmental Research Letters* 20: 34005. https://doi.org/10.1088/1748-9326/adaf44.

Yazbeck, T., G. Bohrer, M. E. Scyphers, et al. 2025. "ELM-Wet: Inclusion of a Wet-Landunit With Sub-Grid Representation of Eco-Hydrological Patches and Hydrological Forcing Improves Methane Emission Estimations in the E3SM Land Model (ELM)." *Journal of Advances in Modeling Earth Systems* 17, no. 2: e2024MS004396.

Yuan, K., F. Li, G. McNicol, et al. 2024. "Boreal–Arctic Wetland Methane Emissions Modulated by Warming and Vegetation Activity." *Nature Climate Change* 14, no. 3: 282–288.

Yuan, K., Q. Zhu, F. Li, et al. 2022. "Causality Guided Machine Learning Model on Wetland CH_4 Emissions Across Global Wetlands." *Agricultural and Forest Meteorology* 324: 109115. https://doi.org/10.1016/j.agrformet.2022.109115.

Zedler, J. B., and S. Kercher. 2005. "Wetland Resources: Status, Trends, Ecosystem Services, and Restorability." *Annual Review of Environment and Resources* 30, no. 1: 39–74.

Zhang, X., L. Liu, T. Zhao, et al. 2023. "GWL_FCS30: A Global 30 m Wetland Map With a Fine Classification System Using Multi-Sourced and Time-Series Remote Sensing Imagery in 2020." *Earth System Science Data* 15, no. 1: 265–293. https://doi.org/10.5194/essd-15-265-2023.

Zhang, Z., S. Bansal, K.-Y. Chang, et al. 2023. "Characterizing Performance of Freshwater Wetland Methane Models Across Time Scales at FLUXNET-CH_4 Sites Using Wavelet Analyses." *Journal of Geophysical Research. Biogeosciences* 128, no. 11: e2022JG007259.

Zhang, Z., E. Fluet-Chouinard, K. Jensen, et al. 2021. "Development of the Global Dataset of Wetland Area and Dynamics for Methane Modeling (WAD2M)." *Earth System Science Data* 13, no. 5: 2001–2023. https://doi.org/10.5194/essd-13-2001-2021.

Zhang, Z., B. Poulter, J. R. Melton, et al. 2025. "Ensemble Estimates of Global Wetland Methane Emissions Over 2000–2020." *Biogeosciences* 22, no. 1: 305–321.

Zhang, Z., N. E. Zimmermann, A. Stenke, et al. 2017. "Emerging Role of Wetland Methane Emissions in Driving 21st Century Climate Change." *Proceedings of the National Academy of Sciences* 114, no. 36: 9647–9652.

Zhou, X., H. Zuo, and S. J. Smaill. 2021. "Incorporation of NPP Into Forest CH_4 Efflux Models." *Trends in Plant Science* 26, no. 12: 1210–1212. https://doi.org/10.1016/j.tplants.2021.09.007.

Zhu, Q., D. J. Jacob, K. Yuan, et al. 2025. "Advancements and Opportunities to Improve Bottom–Up Estimates of Global Wetland Methane Emissions." *Environmental Research Letters* 20, no. 2: 23001.

Zhu, Q., K. Yuan, F. Li, et al. 2024. "Critical Needs to Close Monitoring Gaps in Pan-Tropical Wetland CH_4 Emissions." *Environmental Research Letters* 19, no. 11: 114046.

Zhuang, Q., J. M. Melillo, D. W. Kicklighter, et al. 2004. "Methane Fluxes Between Terrestrial Ecosystems and the Atmosphere at Northern High Latitudes During the Past Century: A Retrospective Analysis With a Process-Based Biogeochemical Model." *Global Biogeochemical Cycles* 18, no. 3: GB3010.

Supporting Information

Additional supporting information can be found online in the Supporting Information section. **Figure S1:** Site-level model performance during training and testing phases. **Figure S2:** Reconstructed daily time series of CH_4 emissions. **Figure S3:** Fractional changes of FCH_4 at 11 sites during summer (June, July, August) and fall (September, October, November) months. **Table S1:** Neural Network architecture defined by hyperparameters.